

The Hubbard model with smooth boundary conditions

M. Vekić* and S.R. White

Department of Physics, University of California Irvine, CA 92717

(June 23, 2021)

Abstract

We apply recently developed smooth boundary conditions to the quantum Monte Carlo simulation of the two-dimensional Hubbard model. At half-filling, where there is no sign problem, we show that the thermodynamic limit is reached more rapidly with smooth rather than with periodic or open boundary conditions. Away from half-filling, where ordinarily the simulation cannot be carried out at low temperatures due to the existence of the sign problem, we show that smooth boundary conditions allow us to reach significantly lower temperatures. We examine pairing correlation functions away from half-filling in order to determine the possible existence of a superconducting state. On a 10×10 lattice for $U = 4$, at a filling of $\langle n \rangle = 0.87$ and an inverse temperature of $\beta = 10$, we did find enhancement of the d -wave correlations with respect to the non-interacting case, a possible sign of d -wave superconductivity.

PACS Numbers: 05.30.Fk, 05.70.Fh, 71.10.+x

I. INTRODUCTION

The two-dimensional (2D) Hubbard model [1] is considered to be one of the possible models to describe the high T_c copper-oxide superconductors [2]. Despite the fact that this model describes quite well the insulating state and some of the normal state properties of the copper-oxides, it is not clear whether it contains all the necessary microscopic features to also explain their superconducting properties [3]. Although a variety of approximate calculations [4–6] predict the existence of superconductivity in the doped Hubbard model, there is still need to find confirmation from a calculation which does not depend on uncontrolled approximations.

Quantum Monte Carlo (QMC) simulations have emerged as a method of choice in trying to solve this model numerically, since, in principle, the interaction is treated in an exact way [7]. The path integral formalism is the standard starting point, where the partition function is decomposed by using the Suzuki-Trotter formula [8]. A widely used algorithm employs the Hubbard-Stratonovich transformation to decouple the interaction and integrate out the fermionic fields [9], leading to a bosonic path integral with an effective action which depends on the fermion determinant given in terms of the bosonic fields only. The trace over the Stratonovich fields can then be replaced by a stochastic sampling in which the fermion determinant becomes essentially the weight of the distribution of Hubbard-Stratonovich fields [10].

However, these simulations have a number of hardware limitations that cannot be easily overcome even with the modern state-of-the-art supercomputers. The first problem is that they can only be implemented on relatively small lattices and at relatively high temperatures, since the computational time increases rapidly with the number of sites of the lattice, and as the temperature is lowered. Thus, ground state properties in the thermodynamic limit can only be obtained via finite-size scaling techniques and zero-temperature extrapolations. The second difficulty is the appearance of the sign problem when the system is doped away from half-filling [11]. The sign problem arises from the fact that the fermion determinant,

which is interpreted as a probability weight of the distribution of Hubbard-Stratonovich fields, is not always positive definite, but decays exponentially with decreasing temperature. Thus, since averages must be computed by taking differences of two positive quantities of similar magnitude, the numerical problem becomes unstable, giving rise to large errors in the measurements. The sign problem in the Hubbard model becomes worse at low temperatures for values of the doping where a possible pairing phase is predicted to exist.

The appearance of these problems has stimulated the search of new techniques for solving Hubbard-like models beyond quantum Monte Carlo simulations [12–14]. In this paper we will instead show that some of the above limitations can be partially overcome using new types of boundary conditions (BCs), *smooth boundary conditions* (SBCs), which have been successfully applied to the study of one-dimensional (1D) systems within a large number of numerical techniques [15]. These BCs consist of *smoothly* decreasing the energy parameters appearing in the Hamiltonian as we approach the edges of the lattice. The result of this operation is that, instead of having a sharp and rigid boundary as is the case with open boundary conditions (OBCs), with SBCs the boundary extends itself into the system in such a way that its exact size is not fully determinable. In general, we will talk of the *bulk* of the system as the region where the energy parameters are constant, and of the *boundary* as the region over which the parameters are smoothly turned off. All measurements are made in the bulk region. In addition to reaching the thermodynamic limit on a relatively smaller system than with periodic boundary conditions (PBCs) or OBCs we find that with SBCs we obtain an improvement in the behavior of the sign problem which allows one to reach significantly lower temperatures and to explore the possible existence of a superconducting phase in the doped system. In Section II we introduce the Hubbard model with SBCs, in Section III we demonstrate the validity of SBCs comparing them to PBCs in the discussion of the half-filled case, in Section IV we describe the behavior of the average sign of the simulation with SBCs and study pairing correlations in the nearly half-filled case, and, finally, in Section V we summarize and conclude.

II. THE MODEL WITH SMOOTH BOUNDARY CONDITIONS

We consider the positive- U Hubbard model [1] on a two-dimensional lattice defined by the Hamiltonian

$$H = - \sum_{\langle ij \rangle, \sigma} t_{ij} (c_{i\sigma}^\dagger c_{j\sigma} + c_{j\sigma}^\dagger c_{i\sigma}) - \sum_{i, \sigma} \mu_i n_{i\sigma} + \sum_i U_i (n_{i\uparrow} - \frac{1}{2})(n_{i\downarrow} - \frac{1}{2}), \quad (1)$$

which consists of a system of itinerant electrons with an on-site interaction of coupling strength U_i . Here t_{ij} is the nearest-neighbor hopping parameter between sites i and j . All the above energy parameters appearing in the Hamiltonian are scaled according to the smoothing function f_i , shown in Fig. 1, in such a way that $U_i/U = \mu_i/\mu = f_i$ and $t_{ij}/t = \frac{1}{2}(f_i + f_j)$, where U , μ , and t are the bulk values. In the following, without loss of generality, we will take $t = 1$, and express all the other parameters appearing in the Hamiltonian of Eq.(1) in dimensionless form. The $c_{i\sigma}^\dagger$ are fermion creation operators in a Wannier orbital centered at site i with spin σ , μ is the chemical potential, and $n_{i\sigma} = c_{i\sigma}^\dagger c_{i\sigma}$ is the density operator.

The above rescaling of the energy parameters in the Hamiltonian is motivated by a similar procedure that was successfully applied to several 1D systems [15]. The choice of the smoothing function f_i emerges from a generalization of the 1D analogue, but is not unique. Here we use $f_i = y(1 - d_i/[N_f + 1])$, where d_i measures the distance of site i from the nearest edge of the system, starting at 1 for i on the outermost “frame”, or square, of sites. N_f is the number of frames in the boundary region. The smoothing function is given by [15]

$$y(x) = \begin{cases} 1 & x \leq 0 \\ \frac{1}{2} \left[1 + \tanh \frac{x-1/2}{x(1-x)} \right] & 0 < x < 1 \\ 0 & x \geq 1. \end{cases} \quad (2)$$

The most important property of the the function $y(x)$ is that it and all its derivatives are continuous everywhere. Thus in the limit of a large number of frames there are no precise interfaces or boundaries which would cause scattering. However, for most of the results shown here, we use $N_f = 2$, and f_i takes on the values 0.817574476 and 0.182425524. A

surprising result of our work is that one can obtain excellent smoothing using only two frames.

III. THE HALF-FILLED CASE

It is well known that the half-filled Hubbard model on an infinite lattice has an anti-ferromagnetic ground state with periodicity commensurate with the lattice [16]. At finite temperature, from symmetry considerations of the antiferromagnetic order parameter, we know that the correlation length remains finite, and, thus, no phase transition occurs. On a finite lattice, however, the behavior is different, since the correlation length can only grow as large as the linear size of the system. Thus, we can still speak of an approximate transition temperature for a finite lattice corresponding to where the correlation length reaches the size of the lattice. This different behavior between a finite and infinite system is very crucial and could lead to the erroneous conclusion that even the infinite system has a finite transition temperature [18]. In general, finite-size effects will be sensitive to the type of BCs used. Thus, it is important to choose BCs which eliminate finite-size effects already on relatively small lattices so that the extrapolation to the infinite system can be taken without the need to consider extremely large lattices.

Despite the fact that the behavior of the half-filled case is well known, we are interested in studying it in the context of SBCs since we want to show that we can obtain thermodynamic limit results on a relatively smaller lattice than when using PBCs. Also, since at half-filling there is no sign problem, we want to show that this effect is independent of the behavior of the average sign with SBCs relative to PBCs. We find that applying SBCs to a finite lattice indeed reduces finite-size effects and allows faster convergence to the thermodynamic limit. We consider two types of measurements, local quantities and correlation functions. We first consider the average kinetic energy per site, given by

$$\langle K_i \rangle = -\frac{1}{4} \left\langle \sum_{j,\sigma} t_{ij} (c_{i\sigma}^\dagger c_{j\sigma} + c_{j\sigma}^\dagger c_{i\sigma}) \right\rangle, \quad (3)$$

where the sum runs over all j nearest neighbors of i . In Fig. 2 we show $\langle K_i \rangle$ as a function of the linear size of the system using PBCs and SBCs. The results for SBCs are obtained with the number of smoothing frames N_f fixed at 2. This means that the bulk will have a linear size that is 4 sites smaller than the corresponding system with PBCs. It is very striking that already on a 6×6 system with a 2×2 bulk region SBCs give a relatively good estimate to the value that we obtain on a 16×16 lattice with PBCs. A similar conclusion can be drawn from Fig. 3, where we show the double occupancy $\langle n_{i\uparrow} n_{i\downarrow} \rangle$. The finite-size effects in this case are much stronger with PBCs than SBCs. Notice that both in Figs. 2 and 3 the measured quantities saturate to the same value for either type of BCs as the system size becomes larger, as expected, since the type of BCs should not have much effect on the behavior of a very large system.

We also consider several other types of local measurements, leading to the same conclusion: *the thermodynamic limit is reached on a smaller lattice with SBCs rather than with PBCs or OBCs*. In Fig. 4 we show the average total energy as a function of the inverse temperature. Also in this case, we see that for each temperature considered, with SBCs we reach the thermodynamic limit more rapidly than with PBCs. This behavior is very similar to what we found in the numerical density-matrix renormalization group (DMRG) study of the spin- $\frac{1}{2}$ Heisenberg chain with SBCs. Also in that case, with SBCs the ground-state energy is reached on smaller lattices than with OBCs [17].

We also examine various correlation functions in order to show that the behavior is similar to that of the local quantities. When using SBCs the correlation functions can only be evaluated for two sites separated by a distance only as large as the size of the bulk. Similarly, with PBCs we can only calculate correlations between points as far out as half the linear size of the system, since the lattice wraps around onto itself. An additional difference is that, since SBCs break the translational invariance of the Hamiltonian, the measurement of local quantities and correlation functions cannot be averaged over the entire lattice, as can be done with PBCs. In this case, the averaging can only be done over sites, or pairs of sites, which are equivalent under the reduced symmetry of the lattice (reflection and

inversion) with SBCs. This implies that, in order to obtain better statistics, we need to run the simulation longer than with PBCs. This is probably the only significant disadvantage of SBCs over PBCs. In Fig. 5 we show the spin-spin correlation function, defined by

$$c(l) = c(l_x, l_y) = \langle (n_{i+l,\uparrow} - n_{i+l,\downarrow})(n_{i,\uparrow} - n_{i,\downarrow}) \rangle. \quad (4)$$

for several systems sizes with PBCs and compare it to the case with SBCs on a 10×10 lattice with two smoothing frames. Again, it appears that with SBCs we can obtain on a smaller system the same results as with PBCs on a considerably larger system. Having shown that the use of SBCs allows one to reduce finite-size effects on relatively small lattices, we now study the effect of SBCs on the average sign by considering the Hubbard model away from half-filling.

IV. THE DOPED SYSTEM

As one dopes the system, the long-range antiferromagnetic order which is present in the ground state of the half-filled band is abruptly destroyed and short-range incommensurate magnetic correlations set in [19]. Here we are mainly interested in studying the possible existence of a superconducting phase away from half-filling. Recently, there has been an enormous effort in trying to obtain the phase diagram of the doped Hubbard model. Most of the studies have not been able to determine conclusively whether there is or there is not a superconducting phase. Approximate techniques have been used, such as self-consistent calculations, mean-field theories and conserving approximations [12], often suggesting the possibility of a parameter regime having d -wave superconductivity. QMC results, which show evidence of an attractive pairing interaction, but no direct evidence of pairing, have not been completely satisfactory because of the appearance of the sign problem already at relatively high temperatures. The possibility exists that the temperature at which the pairing occurs is significantly lower than the accessible temperatures even on as small lattices as an 8×8 .

Although initially we did not expect changing boundary conditions would have a large effect on the average sign, in fact it can. In general, the average sign decays exponentially with the inverse temperature β and system size N , $\langle S \rangle \sim e^{-A\beta N}$ [11], where A depends on the QMC method (determinantal, world-line, projector, *etc.*). If $\langle S \rangle$ falls below about 0.1, it becomes impossible to obtain reasonable results. Previously, we showed that for large values of U the sign decays slower in the world-line method than in the determinantal approach [20]. Here we find that the decay of the average sign can be substantially slower with SBCs than with either open BCs or with PBCs.

In Fig. 6 we show the average sign as a function of inverse temperature for various lattice sizes at a filling of $\langle n \rangle = 0.87$ with $U = 4$ for several types of BCs. If we consider the case with OBCs and PBCs only, we see that on an 8×8 lattice the average sign is already too small at a $\beta \approx 6 - 7$ for calculating measurements accurately. On the other hand, when we consider SBCs we see that the sign allows one to go to lower temperatures even on a lattice as large as a 12×12 with two smoothing frames. In general we find that *the average sign as a function of temperature decays slower with SBCs than with PBCs and OBCs for all values of U* . Particularly suprising is that the smooth system with a *bulk* region of size 4×4 (the solid triangles) has a sign that decays substantially more slowly than either a periodic or open system whose *full* size is 4×4 .

There are several ways in which one can understand why the average sign is better behaved with SBCs rather than with other types of BCs. When we decrease the energy parameters in the Hamiltonian on the edges of the system, we effectively make the local temperature there higher. Thus, smoothing the energy parameters of the system is equivalent to introducing a temperature gradient on the lattice without any heat flow into or out of the bulk of the system. (This strange temperature gradient cannot be realized in a real system, as far as we know.) Thus, if one thought of the average sign as a measurement that is obtained from averaging over the entire lattice, it might be reasonable to expect its behavior to be better with SBCs rather than PBCs. However, the average sign does not really involve some averaging process over the entire lattice—something slightly more subtle

is going on.

However, this point of view can give us some insight into understanding why finite-size effects are much smaller with SBCs rather than with PBCs. Since the boundary is at a relatively higher temperature, a larger number of local states in the Hilbert space are accessible there. Thus, on the boundary, the system has the freedom to choose a larger portion of the Hilbert space, and thus, it can adjust itself in order to satisfy the constraints of the bulk. In the partition function, the lower temperature of the bulk region dominates the high temperature edge region, so the edges adjust to satisfy the bulk.

As mentioned above, the most surprising effect that emerges from Fig. 6 is that the sign on an 8×8 system with SBCs and a 4×4 bulk region is better behaved than on a 4×4 system with OBCs or PBCs. At this point we only have a qualitative argument for this effect. Based on the projector QMC simulation of the same system, we can at least show that this behavior is not completely unexpected. We have verified that the average sign in the projector QMC has a very similar behavior, namely that it is improved with SBCs. In the projector QMC the sign problem originates from the phase of matrix elements (entering in the partition function) of the form,

$$\langle \phi(0) | \phi(\tau) \rangle \equiv \langle \phi(0) | e^{-\tau H} | \phi(0) \rangle, \quad (5)$$

where $|\phi(0)\rangle$ is an initial trial state (which can be, for example, a filled Fermi sea), and $|\phi(\tau)\rangle$ is the initial state propagated to imaginary time $\tau = L\Delta\tau$. The fluctuating Hubbard-Stratonovich fields cause the state $|\phi(\tau)\rangle$ to evolve through Hilbert space, and its precise evolution will depend on the type of BCs used. In particular, with SBCs, in the boundary region, where the temperature is high, the system evolves slowly, so that the propagated state is still very close to the initial state there. The state could evolve rapidly in the bulk region, except for the fact that it is continuously connected to the boundary region. Thus the edges act as a drag force on the bulk, slowing the rapid variations in imaginary time that cause the sign problem.

In order to verify this picture, we studied, using the projector method, a simplified “toy”

model: a 2D non-interacting tight-binding system with the addition of a Ising-like field $\Delta_i = \pm 1$ coupled to the density operator n_i , designed to mimic the Hubbard-Stratonovich field:

$$H = - \sum_{\langle i,j \rangle} t_{ij} (c_i^\dagger c_j + c_j^\dagger c_i) + \sum_i \Delta_i n_i. \quad (6)$$

Two particles were put in the system, since a single particle never has a sign problem. The state of the higher energy particle had a nodal line which moved as the system evolved through imaginary time. If the nodal line rotated through 180° , the system had a minus sign. A specific field configuration was chosen with a spiral configuration through imaginary time to try to drag the particles in a circle in order to get a minus sign as quickly as possible. The field was able to cause rapid rotation of the nodal line in both PBCs and OBCs. In SBCs, however, the nodal line was unable to evolve rapidly on the edges (it was stuck, as if in a viscous fluid), and the part of the nodal line in the bulk was held back. Consequently, it was much more difficult to generate configurations corresponding to minus signs. We believe the results support our picture for the improved behavior of the sign in the interacting system.

We now present local measurements and correlation functions at high enough temperatures to be accessible to both PBCs and SBCs. When comparing the results with the two types of BCs we find similar behavior to the half-filled case. Then we will present results at lower temperatures, inaccessible with PBCs, and continue the analysis with SBCs.

In Fig. 7 we show the kinetic energy as a function of inverse temperature at a filling of $\langle n \rangle = 0.87$, with $U = 4$. With PBCs we can reach only a temperature of $\beta = 6$ on an 8×8 lattice, while with SBCs we can reach $\beta = 12$.

We considered three types of pairing correlation functions, corresponding to different symmetries of the order parameter. In general, a given pairing correlation function is given by

$$D(l) = |\langle \Delta_{i+l} \Delta_i^\dagger \rangle|, \quad (7)$$

where the pairing field operators, Δ_l , are given by

$$\Delta_l^s = c_{l\uparrow}c_{l\downarrow}, \quad (8)$$

for s -wave symmetry, and by

$$\Delta_l^{s^*} = \frac{1}{2}(c_{l\uparrow}c_{l+x\downarrow} + c_{l\uparrow}c_{l-x\downarrow}) + \frac{1}{2}(c_{l\uparrow}c_{l+y\downarrow} + c_{l\uparrow}c_{l-y\downarrow}), \quad (9)$$

and

$$\Delta_l^d = \frac{1}{2}(c_{l\uparrow}c_{l+x\downarrow} + c_{l\uparrow}c_{l-x\downarrow}) - \frac{1}{2}(c_{l\uparrow}c_{l+y\downarrow} + c_{l\uparrow}c_{l-y\downarrow}), \quad (10)$$

for extended s -wave and d -wave symmetry, respectively.

In Fig. 8 we show the pairing correlation functions for the above three different symmetry channels. For all temperatures considered, we find that pairing in a d -wave channel is always an order of magnitude stronger than for an s -wave or extended s -wave channels. Thus, we continue our analysis with the d -wave pairing correlation function only, examine its temperature dependence and compare it to the non interacting case to see whether there is an enhancement with respect to the $U = 0$ case. In Fig. 9 we show the d -wave pairing correlation function for several temperatures with $U = 8$, showing that, as the temperature is decreased there is an enhancement in the pairing. For reference, we also show the corresponding $U = 0$ results to show that there is no enhancement relative to the non-interacting case, for the accessible temperatures. In Fig. 10 we show the d -wave pairing correlation function for lower temperatures with $U = 4$. Here, at $\beta = 10$, we do find evidence for enhancement over the non-interacting case, near the M point. This may be a sign of d -wave superconductivity.

V. CONCLUSIONS

We have implemented a numerical simulation of the 2D Hubbard model using SBCs. We have showed that at half-filling, where there is no sign problem, one obtains thermodynamic limit results on a smaller lattice than when using PBCs. Away from half-filling, we have found that the average sign decays more slowly with inverse temperature and lattice size with

SBCs than with OBCs and PBCs, allowing us to reach significantly lower temperatures and larger lattices. We looked at the pairing correlation functions and showed that the d -wave channel is favored over other types of pairing channels, and that the pairing increases as we lower the temperature. On a 10×10 lattice for $U = 4$, at a inverse temperature of $\beta = 10$, we did find enhancement of the d -wave correlations with respect to the non-interacting case, a possible sign of d -wave superconductivity.

VI. ACKNOWLEDGEMENTS

The authors would like to thank R.M. Noack and R.T. Scalettar for useful discussions. We acknowledge support from the Office of Naval Research under grant No. N00014-91-J-1143. The numerical calculations reported in this paper were performed at the San Diego Supercomputer Center.

REFERENCES

* Marco Vekić passed away on September 20, 1994.

- [1] J. Hubbard, *Proc. Roy. Soc.* **A276**, 238 (1963).
- [2] J.G. Bednorz and K.A. Müller, *Z. Phys.* **B64**, 189 (1986); C.W. Chu *et al.*, *Phys. Rev. Lett.* **58**, 405 (1987).
- [3] A. Moreo *et al.*, *Phys. Rev.***B41**, 2313 (1990).
- [4] P.W. Anderson, *Science* **235**, 1196 (1987).
- [5] J.E. Hirsch, *Phys. Rev. Lett.* **54**, 1317 (1985).
- [6] D.J. Scalapino, E. Loh, and J.E. Hirsch, *Phys. Rev.***B34**, 8190 (1986).
- [7] R. Blankenbecler, D.J. Scalapino, and R.L. Sugar, *Phys. Rev.***D24**, 2278 (1981).
- [8] M. Suzuki, *Prog. Theor. Phys.*, **56**, 1454 (1976).
- [9] J.E. Hirsch, *Phys. Rev.***B28**, 4059 (1983); *Phys. Rev. Lett.* **51**, 1900 (1983); *Phys. Rev.***B33**, 4403 (1985).
- [10] D.J. Scalapino and R.L. Sugar, *Phys. Rev.***B24**, 4295 (1981)
- [11] G.G. Batrouni and R.T. Scalettar, *Phys. Rev.***B42**, 2282 (1990); E.Y. Loh, J.E. Gubernatis, R.T. Scalettar, S.R. White, D.J. Scalapino, and R.L. Sugar, *ibid.* **41**, 9301 (1990).
- [12] N.E. Bickers and S.R. White, *Phys. Rev.***B43**, 8044 (1991); S.R. White *Phys. Rev.***B48**, 10345 (1993); D.J. Scalapino, E. Loh, Jr., and J.E. Hirsch, *Phys. Rev.***B34**, 8190 (1986).
- [13] S.R. White *Phys. Rev. Lett.* **69**, 2893 (1992).
- [14] R.M. Noack, S.R. White, and D.J. Scalapino, (unpublished).
- [15] M. Vekić and S.R. White, *Phys. Rev. Lett.* **71**, 4283 (1993).

- [16] J. Hirsch and S. Tang, *Phys. Rev. Lett.* **62**, 591 (1989); S.R. White *et al.*, *Phys. Rev.***B40**, 506 (1989).
- [17] M. Vekić and S.R. White, (unpublished).
- [18] M. Vekić and S.R. White, *Phys. Rev.***B48**, 7643 (1993).
- [19] H.J. Schulz, *Phys. Rev. Lett.* **64**, 2445 (1990).
- [20] M. Vekić and S.R. White, *Phys. Rev.***B47**, 16131 (1993).

FIGURES

FIG. 1. The smoothing function, $f_i = f_{i_x, i_y}$ for a 12×12 lattice with four smoothing frames. The bulk region is a 4×4 lattice. The four concentric square frames are clearly visible.

FIG. 2. The kinetic energy, $\langle K_i \rangle$, measured at the center of the lattice, as a function of linear system size N_x with $U = 4$ at half-filling at $\beta = 6$. The solid squares are with PBCs and the solid circles with SBCs with two smoothing frames.

FIG. 3. The double occupancy $\langle n_{i\uparrow} n_{i\downarrow} \rangle$, measured at the center of the lattice, as a function of linear system size N_x with $U = 4$ at half-filling at $\beta = 6$. The solid squares are with PBCs and the solid circles with SBCs with two smoothing frames.

FIG. 4. The total energy $\langle E_i \rangle$, measured at a site i in the center of the lattice, as a function of inverse temperature β for several system sizes and with PBCs and SBCs. The filling is $\langle n \rangle = 1$ and $U = 4$. The open symbols are with PBCs and the solid symbols with SBCs. With SBCs we use two smoothing frames on the boundary. The solid lines are just guides to the eye.

FIG. 5. The spin-spin correlation function $c(l_x, l_y)$ at half-filling with $U = 4$ and at $\beta = 6$. The path taken in calculating $c(l_x, l_y)$ is shown in the inset. The solid squares are for a 10×10 system with SBCs and two smoothing frames. The open symbols are with PBCs and on sizes as shown. The solid line is a guide to the eye for the case with SBCs. The errors (not shown) are smaller than the size of the symbols.

FIG. 6. The average sign $\langle S \rangle$ as a function of β with $U = 4$ and at $\langle n \rangle = 0.87$ for different system sizes and BCs. The open symbols are for OBCs and PBCs and the solid symbols are for SBCs for the sizes indicated. The solid lines are just guides to the eye.

FIG. 7. The kinetic energy $\langle K_i \rangle$, measured at the center of the lattice, as a function of β for several systems sizes and with PBCs and SBCs. The filling is $\langle n \rangle = 0.87$ and $U = 4$. The open symbols are with PBCs and the solid symbols with SBCs. The triangles are for an 8×8 and the upside-down triangles for a 10×10 lattices. With SBCs we use two smoothing frames on the boundary.

FIG. 8. The pairing correlation functions $D(l)$ with $U = 4$ at $\langle n \rangle = 0.87$ and at $\beta = 8$. The solid circles are for s -wave, the solid triangles are for extended s -wave, and the solid squares are for d -wave. The path taken through the lattice corresponds to a triangle as indicated in the inset. The corresponding empty symbols are for $U = 0$. The solid lines are just guides to the eye.

FIG. 9. The d -wave pairing correlation function $D^d(l)$ on a 10×10 lattice with $U = 8$ at $\langle n \rangle = 0.87$ for several values of β . The path taken through the lattice corresponds to a triangle as indicated in the inset. The corresponding empty symbols are for $U = 0$.

FIG. 10. The d -wave pairing correlation function $D^d(l)$ on a 10×10 lattice with $U = 4$ at $\langle n \rangle = 0.87$ for several values of β . The path taken through the lattice corresponds to a triangle as indicated in the inset. The solid lines are just guides to the eye. The solid squares are for $\beta = 4$, the solid circles are for $\beta = 6$, the solid triangles are for $\beta = 8$ and the open squares are for $\beta = 10$. The corresponding empty symbols are for $U = 0$.

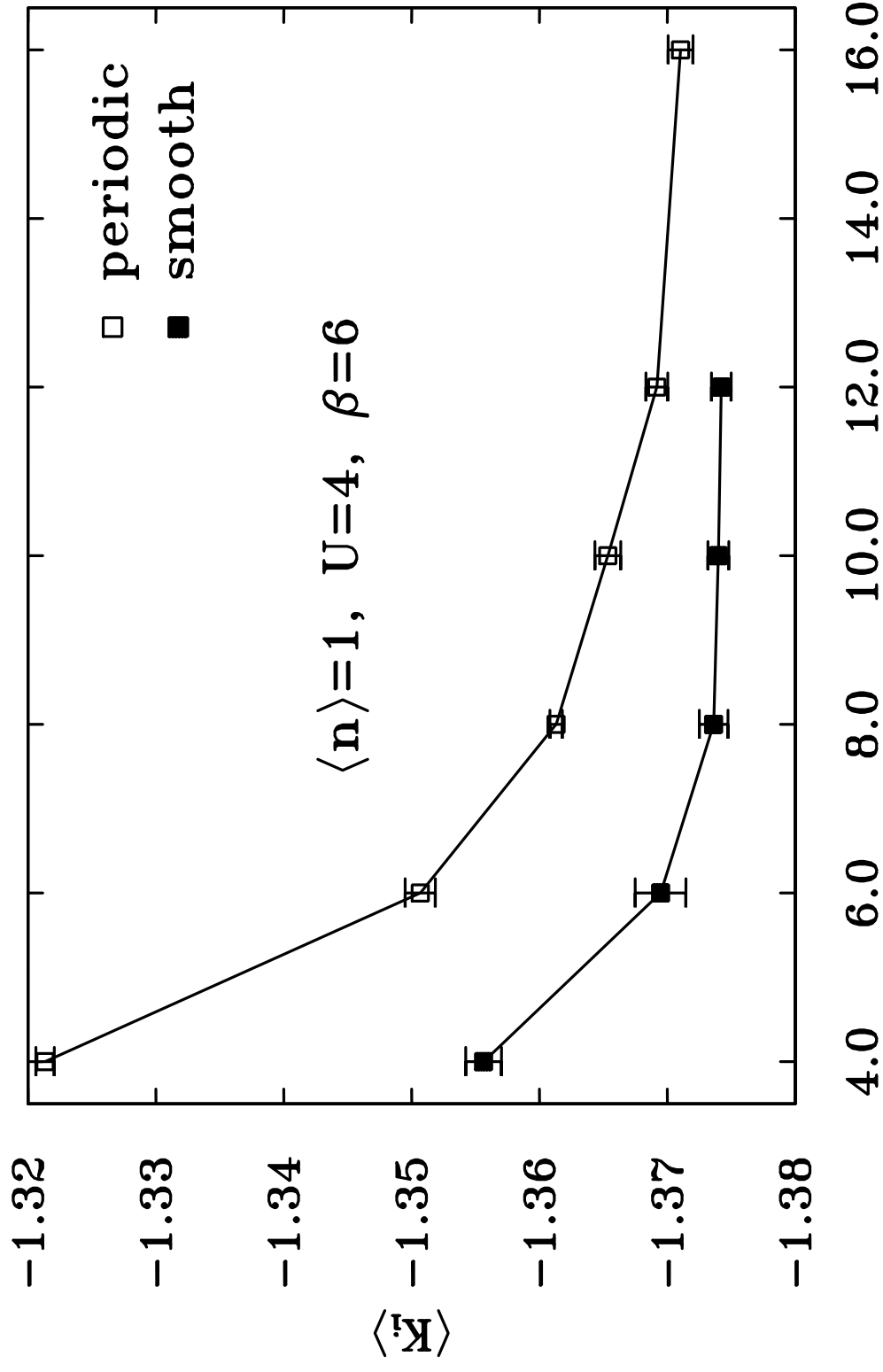


Fig.2

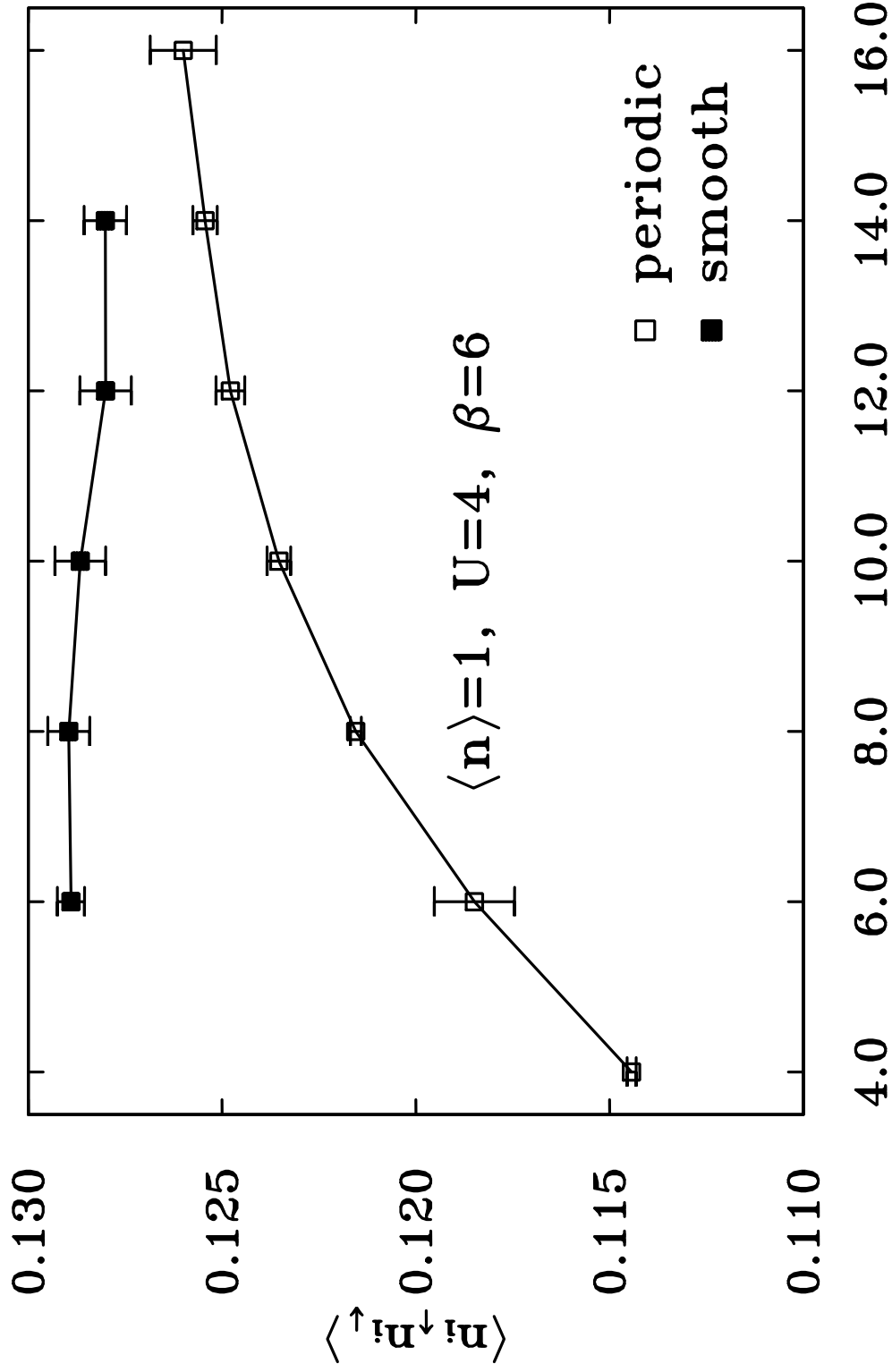


Fig.3

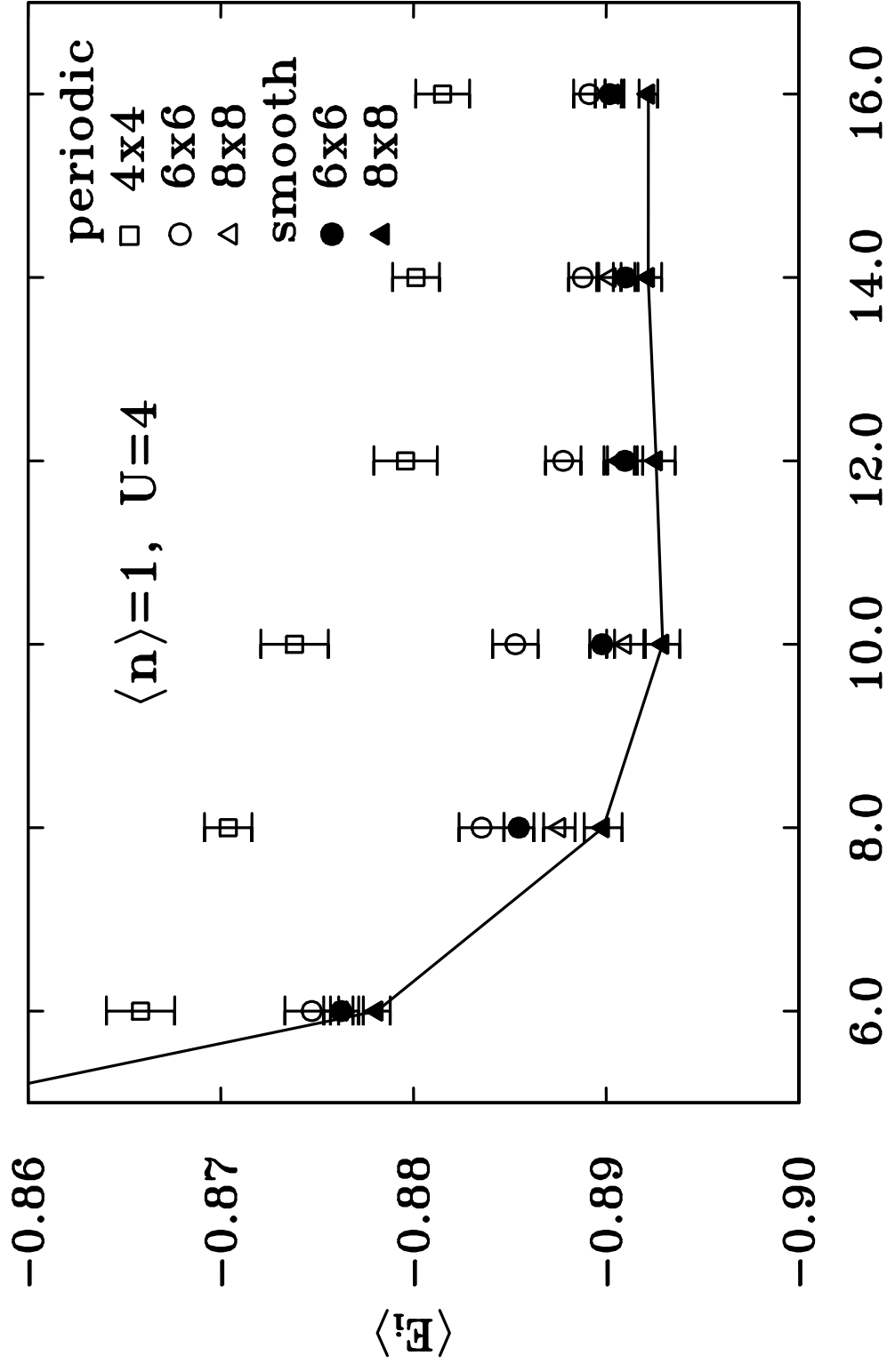


Fig.4

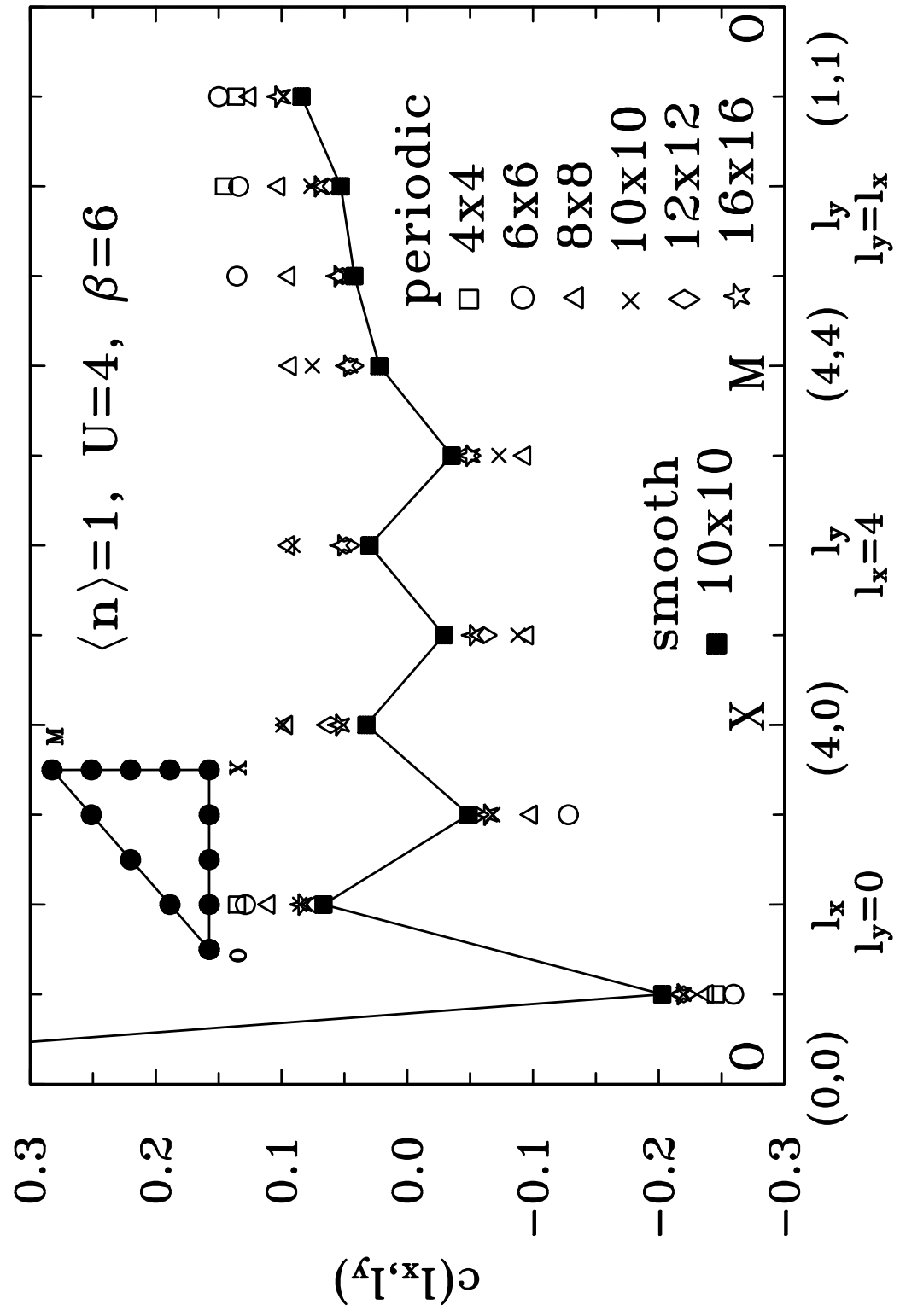


Fig.5

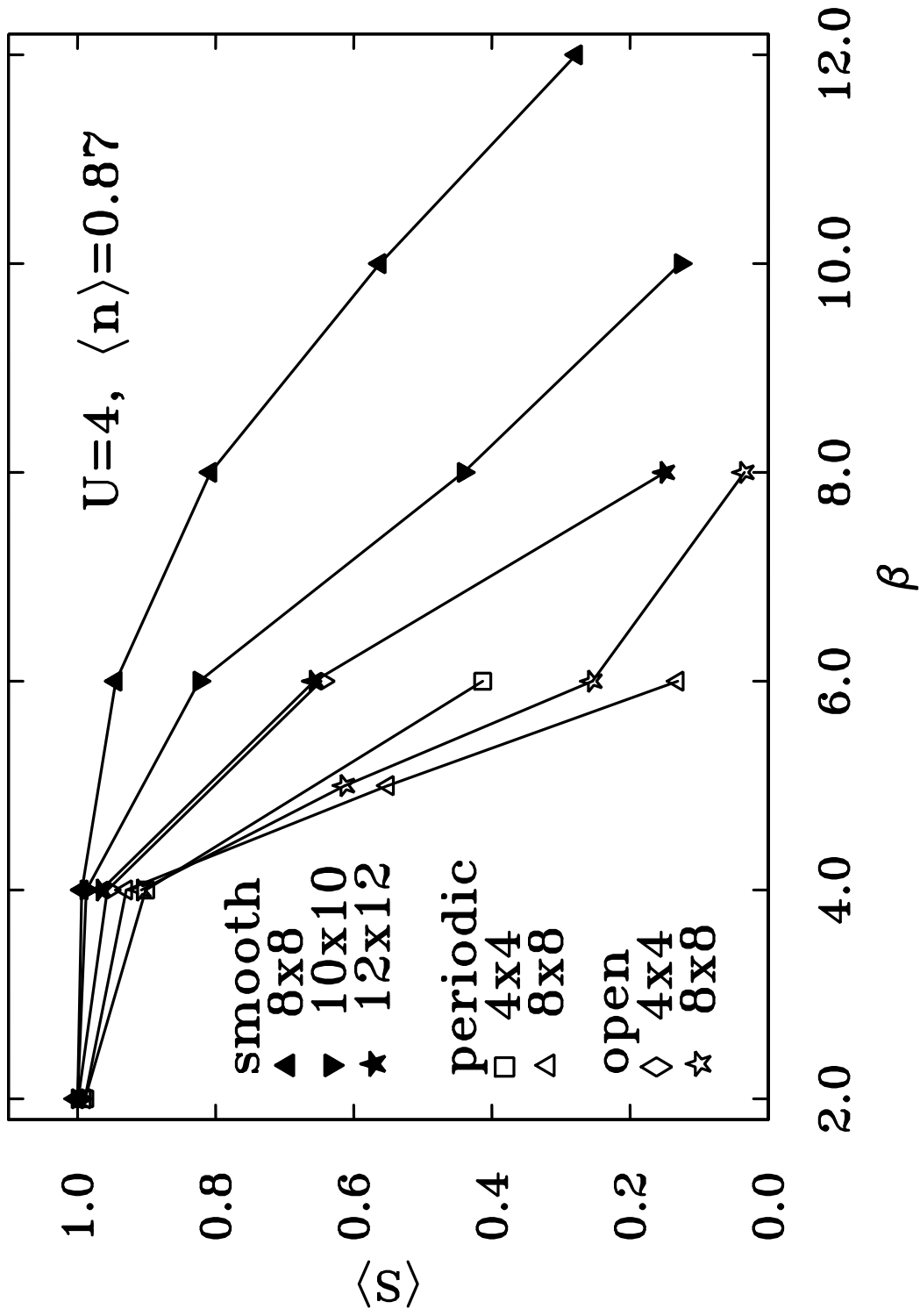


Fig. 6

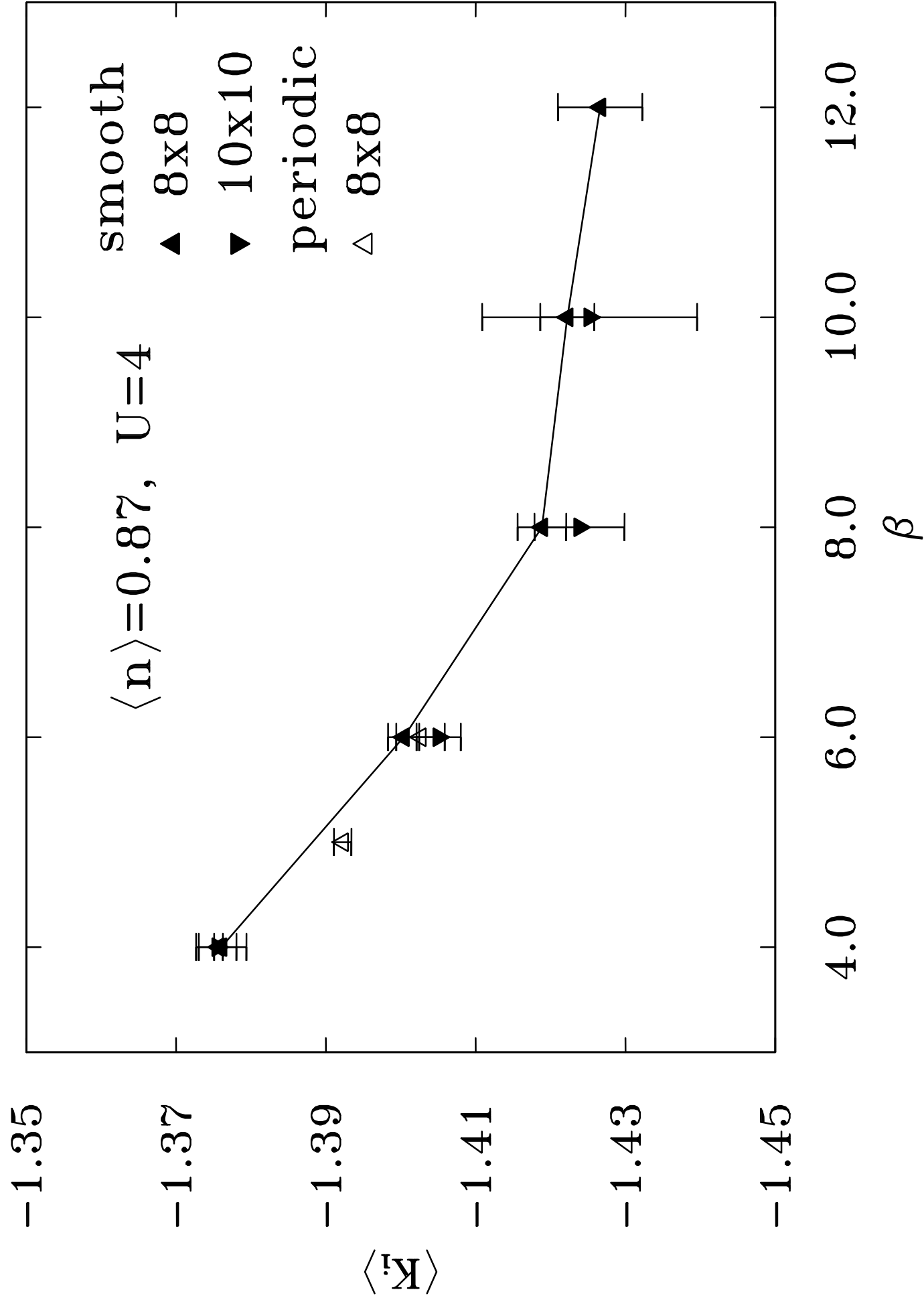


Fig.7

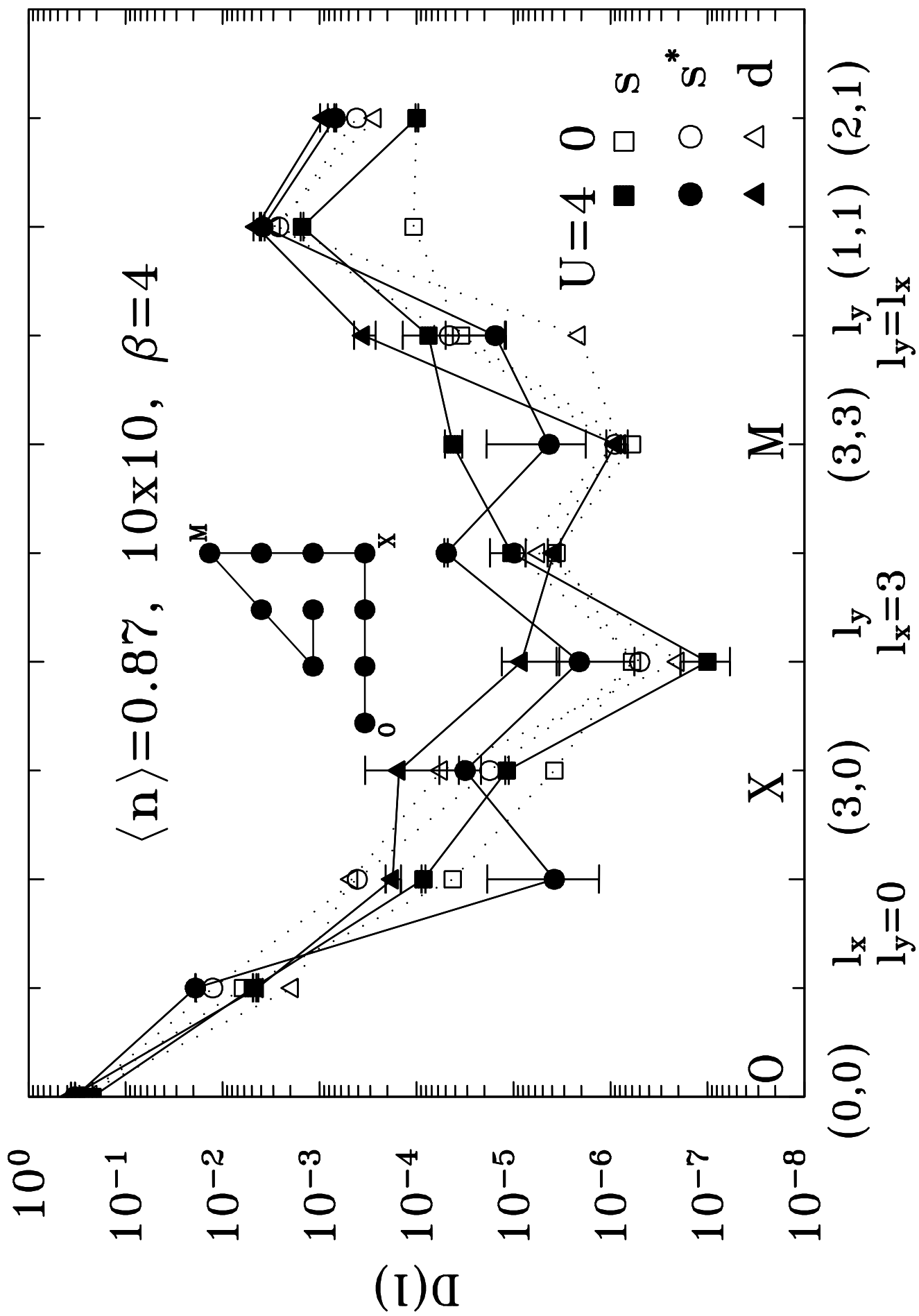


Fig.8

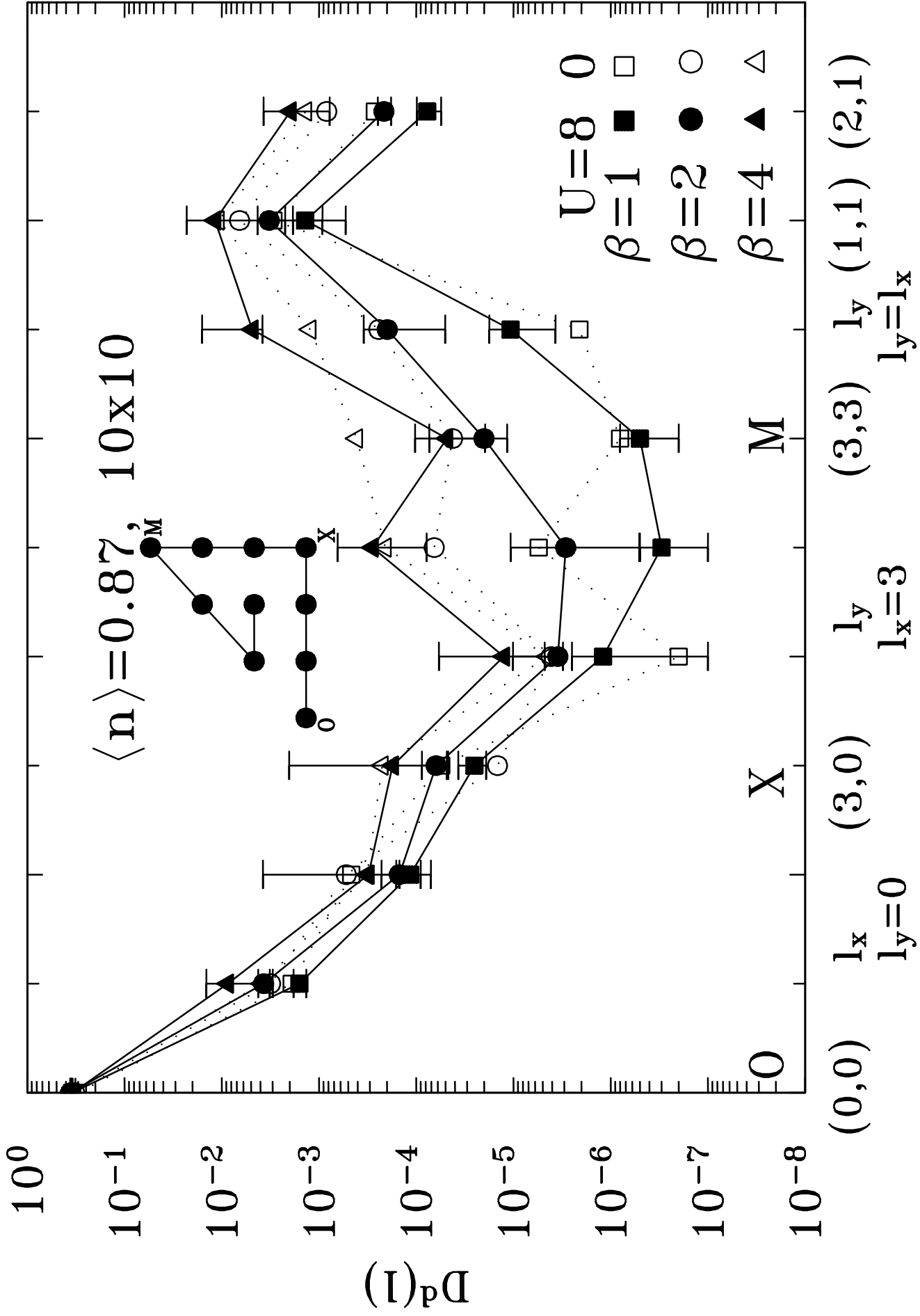


Fig.9

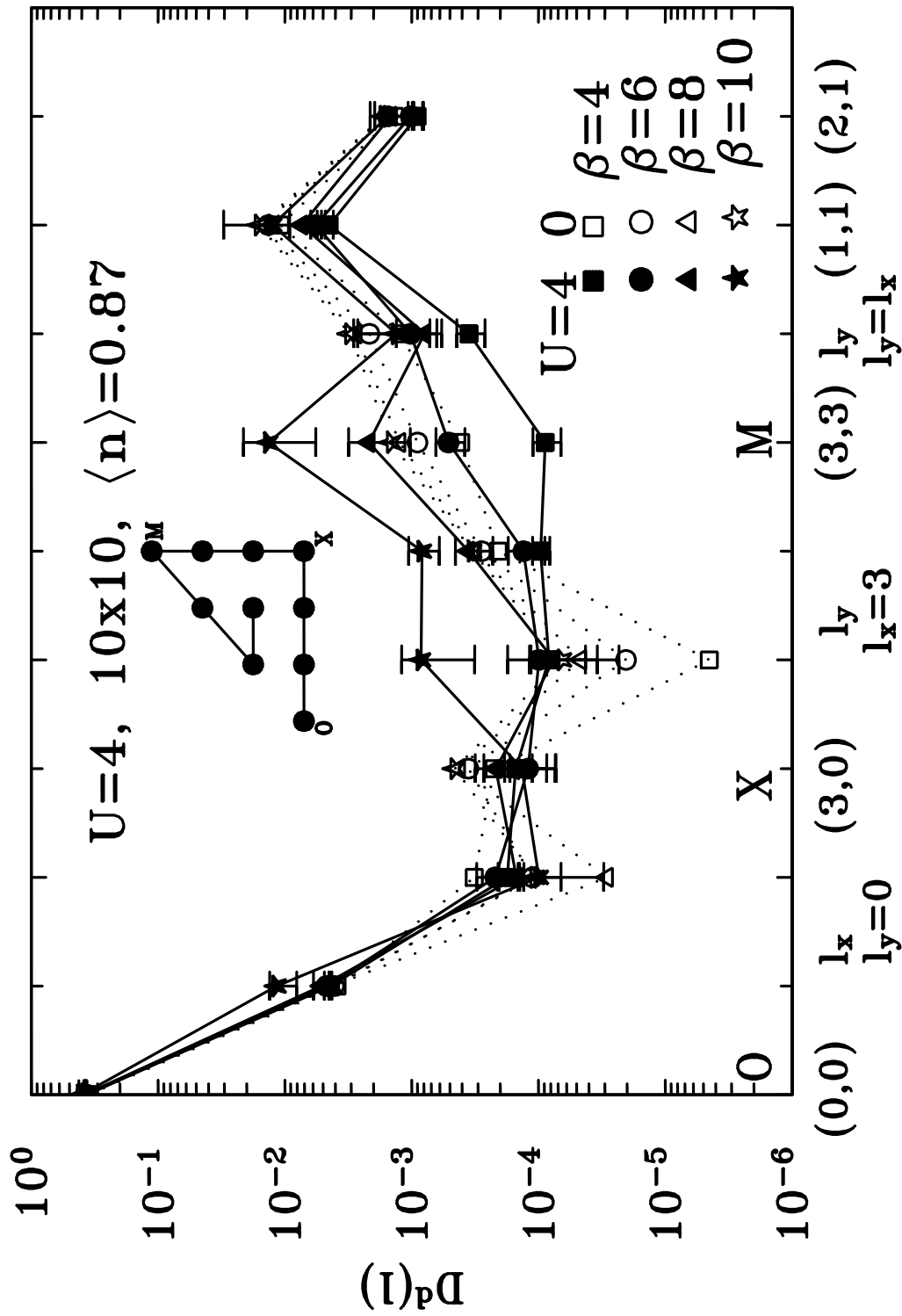


Fig.10